



Experimental Design for the Optimization of the Synthesis Conditions of Zn-Al-Layered Double Hydroxides Nanoparticles Based on X-ray Diffraction Data

Kamellia Nejati, Hassan Keypour, Parvaneh Delir Kheirollahi Nezhad, Karim Asadpour-zeynali & Zolfaghar Rezvani

To cite this article: Kamellia Nejati, Hassan Keypour, Parvaneh Delir Kheirollahi Nezhad, Karim Asadpour-zeynali & Zolfaghar Rezvani (2015) Experimental Design for the Optimization of the Synthesis Conditions of Zn-Al-Layered Double Hydroxides Nanoparticles Based on X-ray Diffraction Data, Molecular Crystals and Liquid Crystals, 608:1, 177-189, DOI: 10.1080/15421406.2014.940261

To link to this article: <http://dx.doi.org/10.1080/15421406.2014.940261>



Published online: 03 Mar 2015.



Submit your article to this journal [↗](#)



Article views: 53



View related articles [↗](#)



View Crossmark data [↗](#)

Experimental Design for the Optimization of the Synthesis Conditions of Zn-Al-Layered Double Hydroxides Nanoparticles Based on X-ray Diffraction Data

KAMELLIA NEJATI,^{1,*} HASSAN KEYPOUR,² PARVANEH DELIR KHEIROLLAHI NEZHAD,¹ KARIM ASADPOUR-ZEYNALI,³ AND ZOLFAGHAR REZVANI⁴

¹Department of Chemistry, Payame Noor University, Tehran, I.R. of Iran

²Faculty of Chemistry, Bu-Ali Sina University, Hamedan, Iran

³Department of Analytical Chemistry, Faculty of Chemistry, University of Tabriz, Tabriz, Iran

⁴Department of Chemistry, Faculty of Basic Sciences, Azarbaijan Shahid Madani University, Tabriz, Iran

This paper demonstrates the synthesis of ZnAl(NO₃)-layered double hydroxide (LDH) nanoparticles based on an experimental design method. The response surface methodology (RSM) was developed as experimental strategies for modeling and optimization of the influence of some variables on the synthesis of LDH. Twenty experiments were carried out for determining the conditions of reactions by the central composite design (CCD) technique. The quantitative variables such as pH, temperature, and reaction time and the qualitative variables including the type of salts and solvents were considered in preparation of LDHs. The responses were average thickness of LDH particles and height of the X-ray diffraction (XRD) patterns.

Keywords Al(NO₃)₃; co-precipitation; experimental design; layered double hydroxide; surface methodology; Zn(NO₃)₂

Introduction

The basic layer structure of layered double hydroxides (LDHs), known as a class of two-dimensional nanostructured anionic clays, can be described as a cadmium iodide-type layered hydroxide (e.g., brucite, Mg(OH)₂) [1] and partial substitution of divalent cations coordinated octahedrally by hydroxyl groups in the layers, by trivalent ones, yielding an excess positive charge, which is balanced by intercalation of anions (usually, water) between the brucite-like sheets [1–4]. These sheets are stacked on top of each other and held together primarily by electrostatic interactions and hydrogen bonds between positive

*Address correspondence to Kamellia Nejati, Department of Chemistry, Payame Noor University, P.O. Box 19395-3697, Tehran, I.R. of Iran. Tel.: +98 411 5412117; Fax: +98 411 5412108. E-mail: nejati.k@yahoo.com, k.nejati@pnu.ac.ir

Color versions of one or more of the figures in the article can be found online at www.tandfonline.com/gmcl.

metal-hydroxide layers and interlayer anions [5,6]. LDHs have relatively weak interlayer bonding and, as a consequence, exhibit excellent ability to capture organic and inorganic anions [1]. The thickness of interlayer region depends on the number, size, and orientation of interlayer anions along with the bond strength between the anions and hydroxyl groups of the brucite-like layers [7]. Also, it is the possibility of varying the identities and relative proportions of the di- and trivalent cations as well as the identity of the interlayer ions over a wide range, which gives rise to a large class of materials having the general formula $[M_{1-x}^{2+}M_x^{3+}(\text{OH})_2]^{x+}[A_{x/n}^{n-}\cdot m\text{H}_2\text{O}]^{x-}$ [2, 8], which belongs to the LDH family, where M^{2+} is a divalent cation, such as Mg^{2+} , Ni^{2+} , Ca^{2+} , Cu^{2+} , Mn^{2+} , Co^{2+} , or Zn^{2+} ; M^{3+} is a trivalent cation, such as Al^{3+} , Cr^{3+} , Ga^{3+} , or Fe^{3+} ; A^{n-} is an interlayer anion, such as CO_3^{2-} , SO_4^{2-} , Cl^- , or NO_3^- [9], and the value of x is equal to the molar ratio of $M^{3+}/(M^{2+}+M^{3+})$ in the range 0.2–0.33 [7]. Note that, altering the trivalent to divalent metal cation ratio will result in the formation of other phases, such as hydroxides and mixed metal oxides [6, 10], with m being the number of water molecules located in the interlayer region together with anions. LDHs represent one of the most technologically promising materials as a consequence of their low cost, relatively easy preparation, large specific surface area, high anion exchange capacity (2–3 meq g^{-1}), which is comparable to those of anion exchange resins, good thermal stability [1, 2], and the large number of composition/preparation variables. The structure of LDH is shown in Fig. 1.

LDHs have recently attracted increasing attention in nano-materials science and technology (NMST) due to their potential application in a wide range of important areas [9], i.e., the catalysis (as catalyst supports, catalysts in important organic reactions, environmental catalysis, catalysts in natural gas conversion, and catalyst precursors) [2, 11–13], medicine (as antiacids, antipeptins, stabilizers, gene and drug delivery vehicles) [14], biochemistry [2, 15], photochemistry [16], electrochemistry (as biosensors based on clay-modified electrodes) [2, 17], anion exchange [18], adsorbents (adsorption of organic and inorganic species) [2, 19], flame retardants [6], electro- and photoactive materials [20], solid-state nanoreactors [21], polymer composites [22], acid residue scavengers, and additives in functional polymer materials [2, 6]. Various methods have been reported to synthesize LDHs as co-precipitates [23], anion-exchanger [24], induced hydrolysis [25], instantaneous precipitation [26], rehydration using structural memory effect, hydrothermal methods, surface

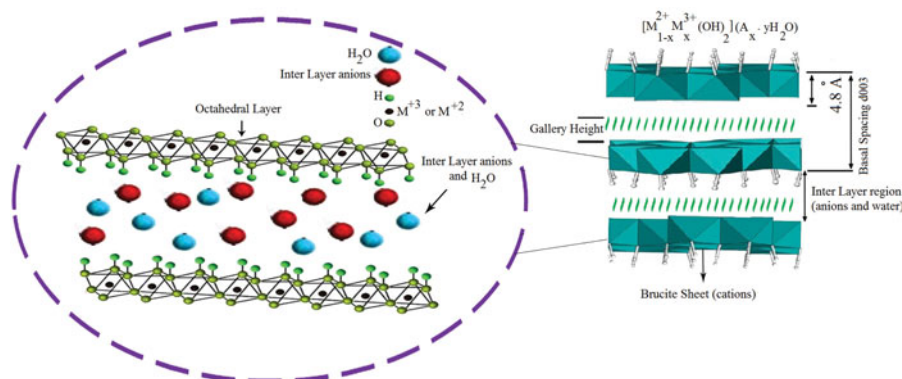


Figure 1. Schematic two- and three-dimensional representation of LDH structure.

synthesis, templated synthesis, and homogenous precipitation with urea [27] in miscellaneous methods including salt oxide method [2, 25]. A wide range of analytical techniques such as the powder X-ray diffraction (PXRD), Fourier transform infrared spectroscopy (FT-IR), thermogravimetry analysis (TGA), differential scanning calorimetry (DSC), scanning electron microscopy (SEM), and the transmission electron microscopy (TEM) has been used in characterization of LDHs. Conventional methods for studying the effects of factors on LDHs synthesis were preliminarily investigated using the one-at-a-time method. One of the disadvantages of this univariate and traditional method is that the best conditions may not be obtained because the interactions between these factors are neglected. In most cases, however, these factors may be completely interdependent. Moreover, the number of experiments needed to reach the global optimum may be impractically large. Thus, experimental methods are preferred approaches for finding the influence of each parameter and their interactions and obtaining the global optimum conditions. To the best of our knowledge, current experimental design has not been applied for optimization of LDH synthesis conditions elsewhere.

The aim of this work is the synthesis and characterization of $\text{ZnAl}(\text{NO}_3)\text{-LDH}$. In producing nanoparticles of LDH, the reaction time (R_t), the temperature (T), and pH were taken as variable factors in the synthesis. Central composite design (CCD) and response surface methodology (RSM) were used for better understanding of relationships between the mentioned parameters with the average thickness of LDH particles and the optimal conditions for $\text{ZnAl}(\text{NO}_3)\text{-LDH}$ synthesis. The synthesized LDHs were subsequently characterized using PXRD, FT-IR, TGA, SEM, and TEM techniques.

Experiment

Materials

$\text{Zn}(\text{NO}_3)_2 \cdot 6\text{H}_2\text{O}$, $\text{Al}(\text{NO}_3)_3 \cdot 9\text{H}_2\text{O}$, and other reagents were all of analytical grade (A.R.) and used as received without further purification (all chemical reagents purchased from Merck Chemical Company, Germany). Water was deionized and CO_2 -free.

Preparation of $\text{ZnAl}(\text{NO}_3)\text{-LDH}$ by the Co-precipitation Method

LDHs containing Zn and Al were prepared from $\text{Zn}(\text{NO}_3)_2 \cdot 6\text{H}_2\text{O}$ and $\text{Al}(\text{NO}_3)_3 \cdot 9\text{H}_2\text{O}$ with the experimental $\text{Zn}^{+2}/\text{Al}^{+3}$ ratio of 3.0 at different pH, temperatures, and reaction times by a co-precipitation method, as described in the literature [28, 29], with slight modifications, in a mixed distilled water and 1-propanol solvent system and ethylene glycol being used as a surfactant. An NaOH solution (0.5 M) was added dropwise into a 35 mL solution containing $\text{Zn}(\text{NO}_3)_2 \cdot 6\text{H}_2\text{O}$ (0.0018 mol) and $\text{Al}(\text{NO}_3)_3 \cdot 9\text{H}_2\text{O}$ (0.0006 mol) in a mixture of distilled water (25 mL), 1-propanol (5 mL), and ethylene glycol (5 mL) under a nitrogen atmosphere with vigorous magnetic stirring until the final pH of 7.5.

Then, the resulting slurry was aged about 1 hr at room temperature and then transferred into a Teflon-lined autoclave and then hydrothermally treated at 120°C for 18 hr. The obtained precipitates were recuperated by filtration, washed several times with distilled water to remove any ions possibly remaining in the final products, and dried at 80°C in a vacuum. This reaction was repeated at different conditions of pH, temperature, and reaction time.

Table 1. The variables and values used for central composite design in LDH synthesis

Number of factors	Factors	Levels of factors ($\alpha = 2$)				
		−2	−1	0	+1	+2
1	Reaction time (R_t)	14	18	22	26	30
2	Temperature (T)	30	60	90	120	150
3	pH	6	7.5	9	10.5	12

Experimental Design

Statistical Analysis for Central Composite Design (CCD)

The statistical software package Minitab version 14 (Minitab Ltd., Coventry CV3 2TE, UK) was used for experimental design, analysis, and optimization. The RSM was employed, using the CCD [30]. Three variables were used in the study, namely, reaction time (R_t), temperature (T), and pH. The conditions that were kept constant for each experiment run were the type of salts, $\text{Zn}^{+2}/\text{Al}^{+3}$ and the solvents ratios. According to previous experiences, when ZnAl-LDHs are synthesized with $\text{Zn}^{+2}/\text{Al}^{+3}$ ratio 3 in a mixture of distilled water, 1-propanol, and ethylene glycol, the LDHs lead to better morphology, crystallinity, and thickness of particles. Hence, for each of the three studied factors, a five levels ($-\alpha$,

Table 2. Different conditions of preparation of LDHs

Run	pH	T (°C)	R_t (hr)	Average thickness of LDH particles (nm)	Height of the d_{003} diffraction peak (a. u)
1	7.5	120	26	19.45	248.0
2	9.0	90	22	12.38	119.2
3	10.5	120	18	9.60	142.0
4	9.0	90	30	17.38	88.7
5	7.5	120	18	19.75	240.0
6	9.0	90	22	12.38	119.2
7	10.5	60	26	32.66	64.0
8	7.5	60	26	6.13	83.0
9	9.0	90	22	11.28	81.0
10	9.0	90	22	10.47	95.9
11	9.0	90	22	14.00	112.5
12	10.5	120	26	9.16	141.5
13	9.0	90	14	12.44	80.5
14	7.5	60	18	12.98	84.8
15	10.5	60	18	32.45	63.5
16	9.0	90	22	10.47	95.0
17	6.0	90	22	15.59	58.0
18	12.0	90	22	16.00	112.0
19	9.0	30	22	17.20	84.0
20	9.0	150	22	9.10	141.0

$-1, 0, +1, +\alpha$) design in low and high ($\alpha = 2$) set points were selected as shown in Table 1.

The analyzed responses were the average thickness of LDH particles and height of the X-ray diffraction (XRD) patterns. The optimal conditions of the factors were obtained by analyzing surface plots. The statistical analysis of the model is represented in the form of analysis of variance (ANOVA) analysis. Table 2 shows 20 runs of the three factors, each at five levels. The design was constructed from eight factorial points, six axial points, and six replications at the central point. In each run, the average thickness of the LDH platelets was calculated through the Scherrer equation and along with height of the d_{003} diffraction peak was used as responses.

The second-order polynomial equation for the variables is as follows:

$$Y = \beta_0 + \beta_1 pH + \beta_2 T + \beta_3 R_t + \beta_4 pH^2 + \beta_5 T^2 + \beta_6 R_t^2 + \beta_7 pH \cdot T + \beta_8 pH \cdot R_t + \beta_9 T \cdot R_t$$

where Y is the response variable, β_0 is a constant, $\beta_1 - \beta_9$ are coefficients for the linear, quadratic, and higher-order interaction effects, respectively. pH , T , and R_t were taken as independent variables. The above quadratic equation was used to plot surfaces for all variables. In order to find the significant and important factors for building a model to optimize the synthesis procedure, a model including all terms in above equation was employed. Then, by the back elimination process, the terms that were not significant were eliminated. Such terms include the variables or interactions that had no insignificant effect on the response.

The selection of optimal conditions is possible from the response surface plots (Figs. 2 and 3) and the obtained model (coefficient was not shown here).

Characterization of LDHs

The PXRD patterns of prepared samples were recorded on a Bruker AXS model D8 Advance diffractometer using $\text{Cu-K}\alpha$ radiation ($\lambda = 1.542 \text{ \AA}$), with the Bragg angle ranging from 4° to 70° . The FT-IR spectra were obtained on a Shimadzu 8400 s spectrophotometer in the range of $4000\text{--}400 \text{ cm}^{-1}$ using the KBr pellet technique. The morphology of the samples was investigated using SEM (LEO 440i, at 20 keV) and TEM (Cambridge, stereo scan 360, 1990, 100 kV accelerating voltage). Zn and Al contents of the samples were determined using an atomic absorption (Varian AA 220, including Zeeman) instrument after dissolving the samples in nitric acid. The TGA was carried out on a Mettler-Toledo TGA 851e apparatus at a heating rate of $10^\circ\text{C min}^{-1}$ under the nitrogen atmosphere.

Results and Discussion

The main goal of this study was finding the optimum conditions for the synthesis of LDH nanoparticles based on the experimental design method. The effects of reaction time, temperature, and pH on $\text{ZnAl}(\text{NO}_3)\text{-LDH}$ synthesis were studied using the RSM. Total of 20 runs were performed to study the effects of mentioned parameters on the average thickness of particles and the height of the d_{003} diffraction peak. Therefore, in this design, the responses for optimization were average thickness of LDHs and the height of the d_{003} diffraction peak. The experimental design and their responses are summarized in Table 2.

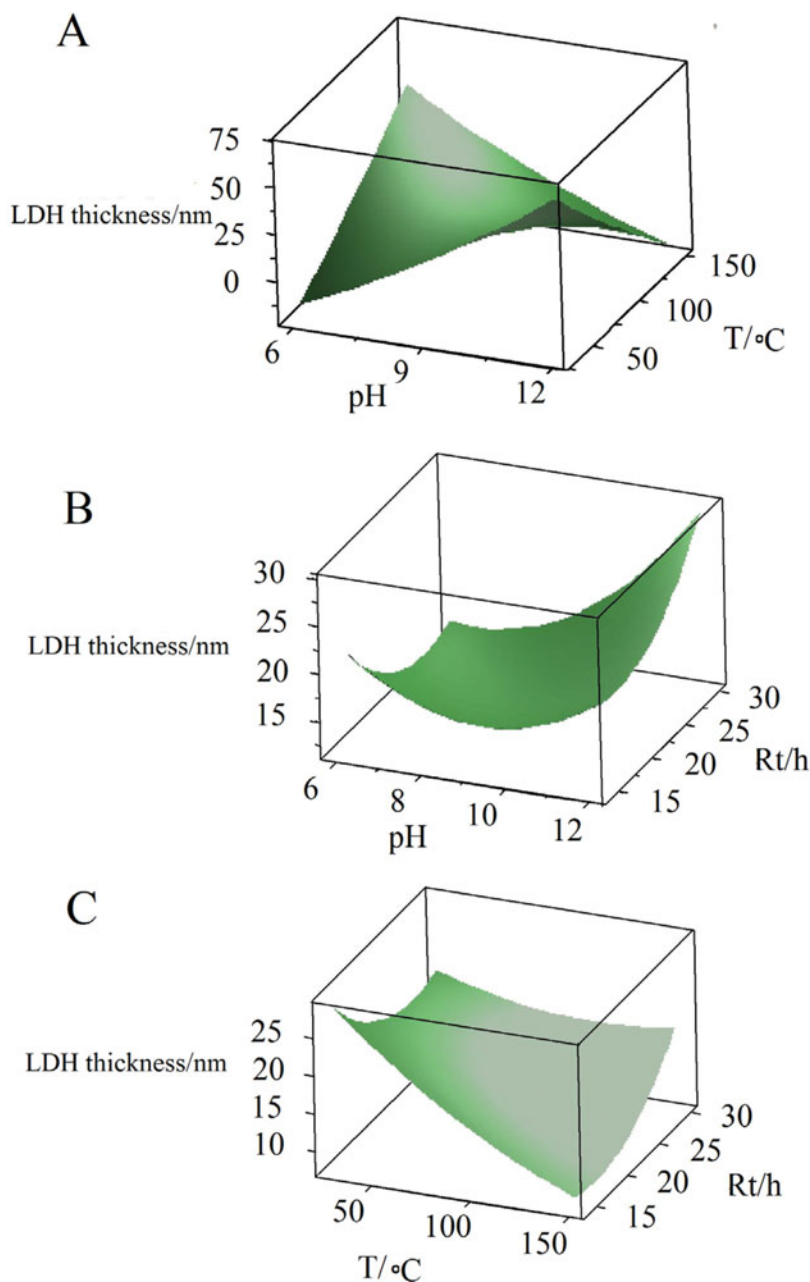


Figure 2. Plot of LDH thickness versus two factors: effects of pH and T (A), pH and R_t (B), and T and R_t (C) on average thickness of LDH particles.

Figure 2 shows the three-dimensional surfaces plots of LDH thickness versus two factors. This figure illustrates relationships between factors and response and is used to obtain an exact optimum. Figure 2A shows the effects of pH and T on the thickness of LDH. The factors pH and T are observed to have different effects on the thickness of LDH.

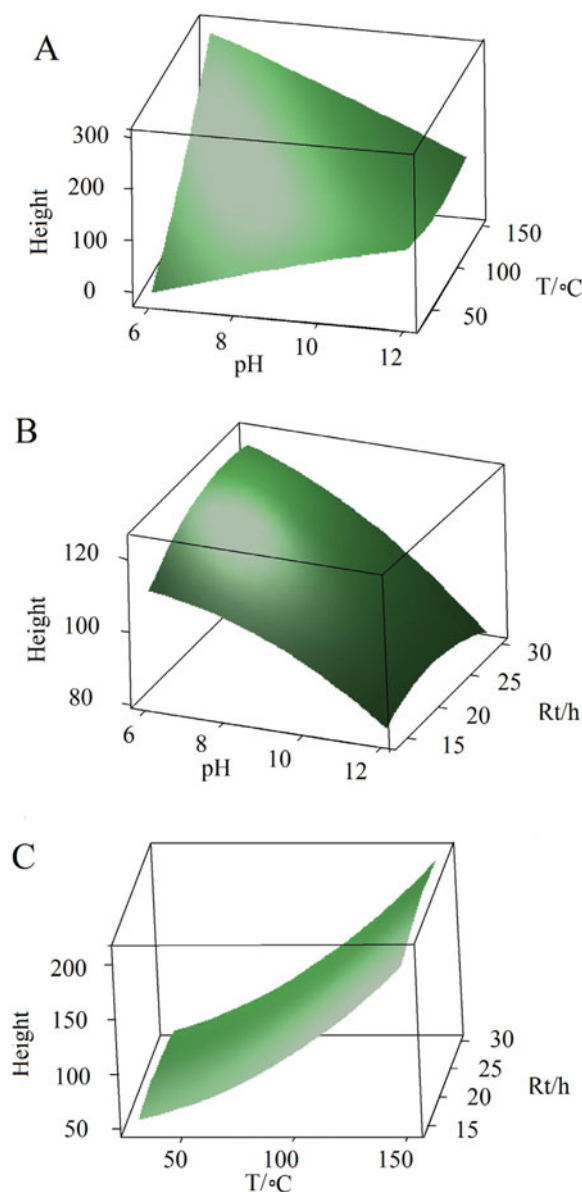


Figure 3. Plot of height of the d_{003} diffraction peak versus two factors: effects of pH and T (A), pH and R_t (B), and T and R_t (C) on height of the d_{003} diffraction peak of LDH.

It means that there is interaction among pH and T . In Fig. 2B, the effect of two parameters including pH and R_t is investigated. The best or minimized response for LDH thickness is observed at pH = 7.5, $T = 120^\circ\text{C}$, and $R_t = 18$ hr. Figure 2C shows the plot of response versus two factors T and R_t on the thickness of LDH nanoparticles. From Fig. 2C it becomes known that thickness of LDH is minimum when $T = 120^\circ\text{C}$ and $R_t = 18$ hr. The same optimum conditions were obtained when the response was the height of the d_{003} diffraction

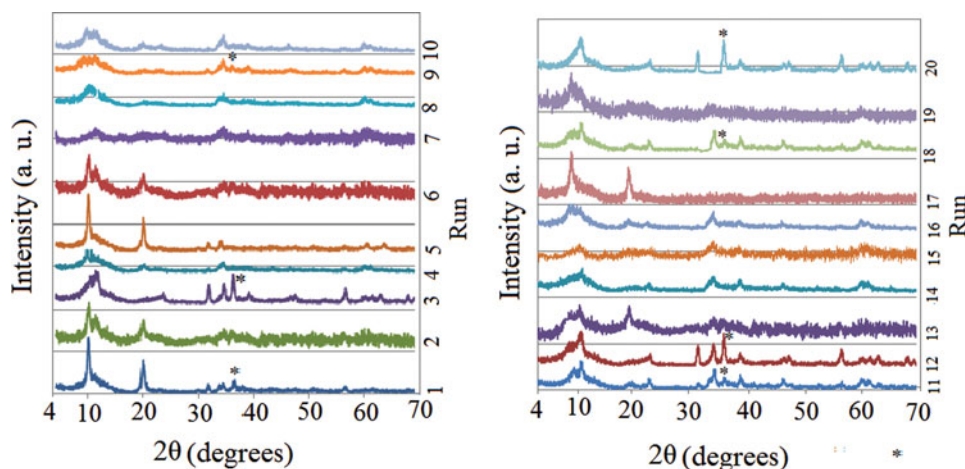


Figure 4. XRD patterns of all samples (* is related to ZnO phase).

peaks. The surfaces were shown in Fig. 3. In this case, the optimum conditions are obtained when peaks are the highest.

The LDHs were characterized by PXRD in the range of $2\theta = 4^\circ\text{--}70^\circ$, where the expected d_{003} peak characteristic of the diffraction pattern of layered solids was recorded [31]. The corresponding XRD patterns for all samples are shown in Fig. 4.

The quality of the LDHs can be detected by the intensity and sharpness of diffraction peaks. The XRD patterns of sample 5, show a pure crystalline LDH phase with narrow, strong, and symmetrical peaks at low 2θ values and fit well to LDH with basal reflections of the hkl planes (003), (006), (009), (015), (110), and (113) at $2\theta = 10.5^\circ$, 21° , 32° , 34° , 60° , and 62° [32–35]. The $2\theta = 60^\circ$ line is also a characteristic of the hydrotalcite structure [36]. The absence of crystalline or amorphous impurities (i.e., zinc oxide (ZnO) or bayerite ($\text{Al}(\text{OH})_3$)) was also determined [6]. The patterns present strong lines positioned in crystallographic indices (003) and (110) allow for the calculation of the lattice parameters “c” ($3d_{003}$) and “a” ($2d_{110}$), respectively, if a hexagonal packing structure is assumed. In particular, the width of the d_{003} diffraction peak was used to estimate the average thickness of the LDH platelets (D) through the Scherrer equation, which is suitable for crystallite thickness ranging from 3 to 200 nm [37].

$$D = K\lambda/\beta \cos \theta$$

where K is the shape factor of the average crystallite (expected shape factor is 0.94) [38], λ is the wavelength ($\lambda = 1.542 \text{ \AA}$ for Cu- K_α), θ is the Bragg’s angle in degree unit, and β is the full width at half maximum of the XRD peak. The XRD patterns of the other samples indicate that, furthermore low crystallinity, besides $\text{ZnAl}(\text{NO}_3)\text{-LDH}$, about some samples, an additional second zinc oxide phase formed on the surface of the brucite-like sheets is present [6, 31]. These results show that the preparation conditions of $\text{ZnAl}(\text{NO}_3)\text{-LDH}$ sample 5 as pH 7.5, temperature 120°C , and reaction time 18 hr, help in obtaining compound with high crystallinity and purity in other conditions. The estimated average thickness from XRD data for all samples is provided in Table 2.

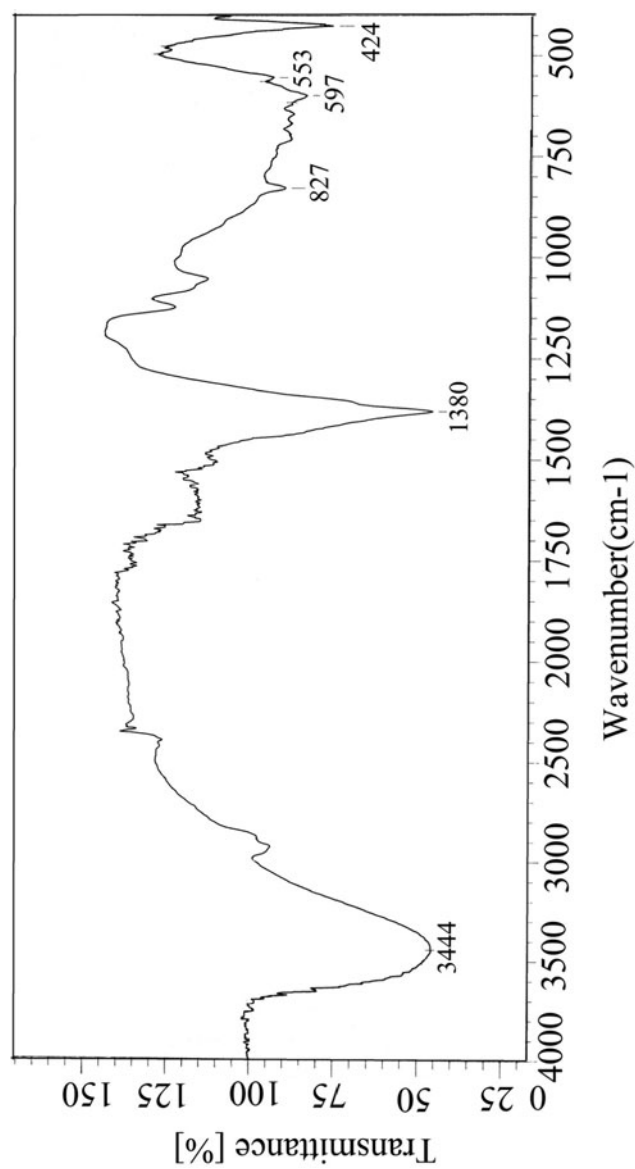


Figure 5. FT-IR spectra of sample 5.

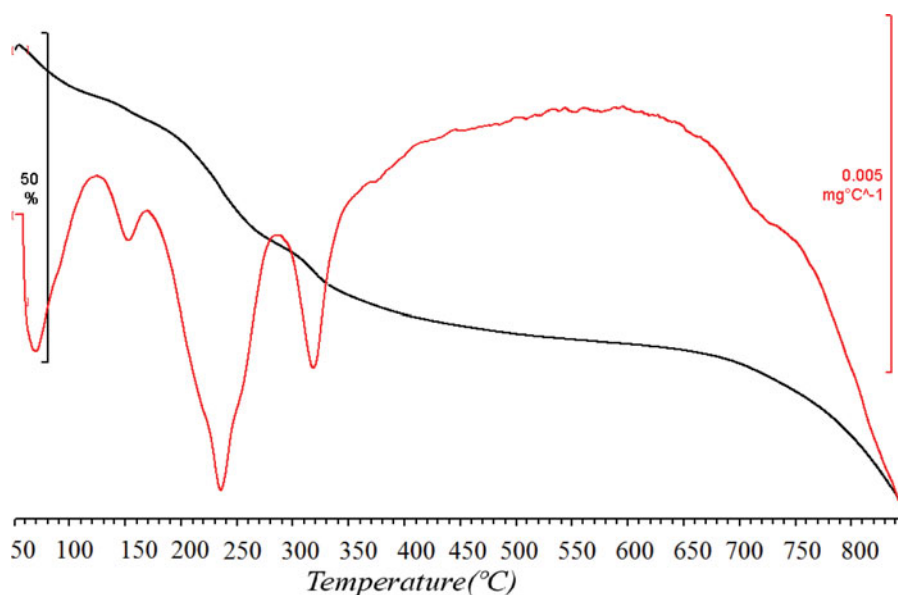


Figure 6. TG-DTG thermograms of sample 5.

FT-IR spectra of sample 5 nanoparticles at room temperature are presented in Fig. 5. The broad absorption band around 3444 cm^{-1} is due to the O–H stretching vibration of the metal hydroxide layer and interlayer water molecules. Absorption at 1380 cm^{-1} is related to the ν_3 vibration of NO_3^- [39]. Also, the weaker band at 1629 cm^{-1} is due to O–H bending deformations. In the low-frequency region, three bands at 597 , 553 , and 424 cm^{-1} are ascribed to the lattice vibration modes attributed to M–O and O–M–O vibrations [40].

The thermal behavior of $\text{ZnAl}(\text{NO}_3)\text{-LDH}$ sample 5 is investigated by using the TG analysis. These TG-DTG curves are depicted in Fig. 6.

The two first and second steps at low temperatures (50°C – 160°C) correspond to the water loss from internal gallery surfaces and the external non-gallery surfaces. The third step observed at higher temperature (240°C) is mainly attributable to the dehydroxylation of the brucite-like octahedral layers in $\text{ZnAl}(\text{NO}_3)\text{-LDH}$ [35]. The fourth step observed above 300°C is due to the elimination of NO_3^- intercalated in the LDH interlayers [41].

The SEM and TEM images of the sample 5 dispersions are shown in Fig. 7. As it is observed in Fig. 7, LDH has plate-like particles with roughly hexagonal shapes when observed using SEM and TEM.

Table 3. Results from the thermogravimetry (TG) analysis and the atomic adsorption spectrometer (AAS)

Sample	Zn(wt%)	Al(wt%)	H(wt%)	N(wt%)	Chemical formula
$\text{ZnAl}(\text{NO}_3)\text{-LDH}$	40.93	5.95	2.88	3.08	$\text{Zn}_{0.74}\text{Al}_{0.26}(\text{OH})_2\text{-(NO}_3\text{)}_{0.26}\cdot 0.70\text{H}_2\text{O}$

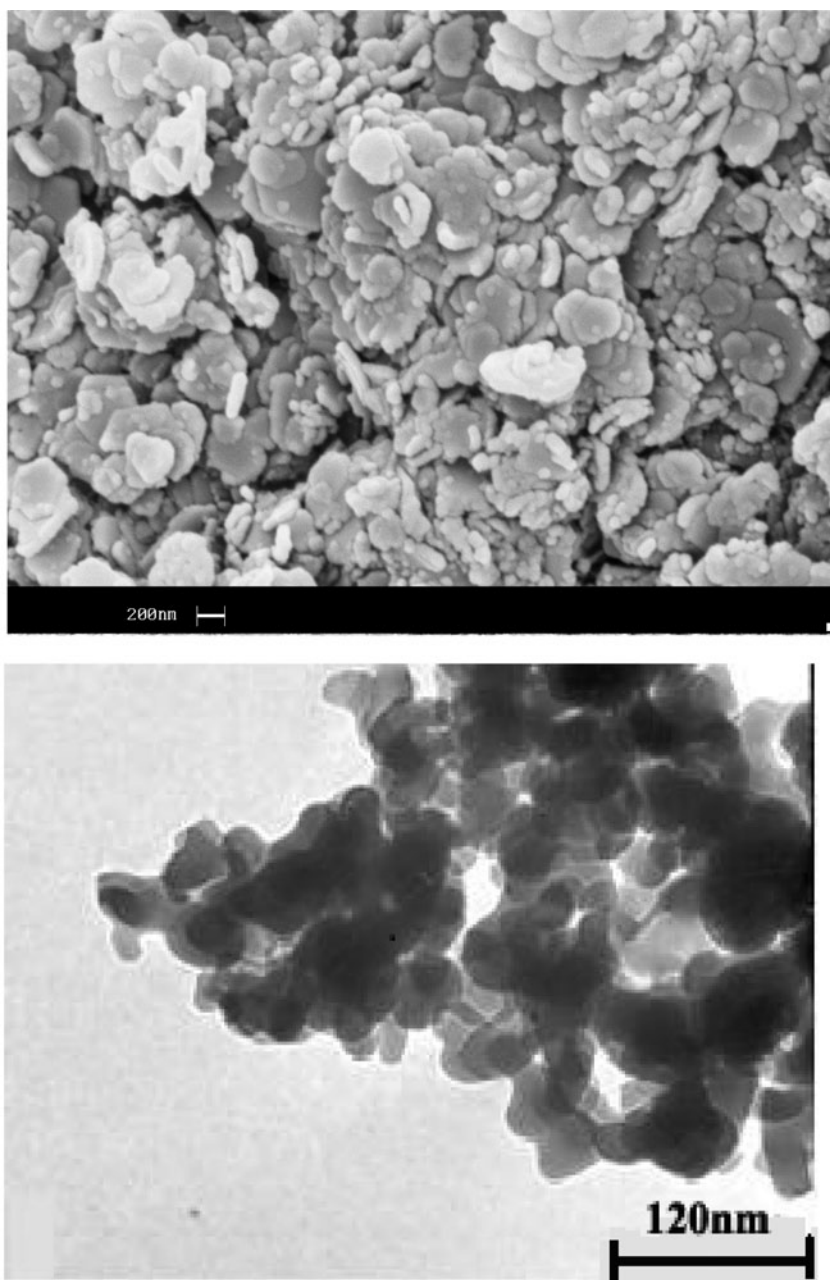


Figure 7. SEM and TEM images of sample 5.

The sample 5 was further analyzed for Zn, Al, H, and N content for the composition of the hydrotalcite layers. It should be noted that the determination of the chemical composition of LDH was the results of elemental analysis and TG analysis (for amount of water) and the role of charge balance. These results are summarized in Table 3. From this table, the molecular formula of the $\text{ZnAl}(\text{NO}_3)\text{-LDH}$ could be determined as $\text{Zn}_{0.74}\text{Al}_{0.26}(\text{OH})_2(\text{NO}_3)_{0.26}\cdot 0.70\text{H}_2\text{O}$.

Conclusion

The nanoparticles of ZnAl(NO₃)-LDH with molar ratio of 3:1 were synthesized from Zn(NO₃)₂·6H₂O and Al(NO₃)₃·9H₂O by a co-precipitation method. Twenty experiments were performed and the RSM was employed, using a CCD for modeling and optimization of the influence of three variables of pH, temperature, and reaction time on the synthesis of ZnAl(NO₃)-LDH. The type of the salts, the Zn⁺²/Al⁺³ ratio, and solvents were kept constant. The responses were average thickness of LDH particles and height of the XRD patterns. The best response for average thickness of LDH particles was observed at pH = 7.5, *T* = 120°C, and *R_t* = 18 hr. The synthesized LDHs were characterized using PXRD, FT-IR, TGA, SEM, and TEM techniques.

Funding

The authors thank the Payame Noor University-Tabriz Center for the financial support of project.

References

- [1] Goh, K.-H., Lim, T.-T., & Dong, Z. (2008). *Water Res.*, 42, 1343.
- [2] Duan, X., & Evans, D. G. (2006). *Layered Double Hydroxides*, Springer: New York.
- [3] Zhang, F., Xiang, X., Li, F., & Duan, X. (2008). *Catal. Surv. Asia*, 12, 253.
- [4] Shan, D., Yao, W., & Xue, H. (2007). *Biosens. Bioelectron.*, 23, 432.
- [5] Auerbach, S. M., Carrado, K. A., & Dutta, P. K. (2004). *Handbook of Layered Materials*, CRC Press: Boca Raton, FL.
- [6] Musumeci, A., Xu, Z., Smith, S., Minchin, R., & Martin, D. (2010). *J. Nanopart. Res.*, 12, 111.
- [7] Cavani, F., Trifirò, F., & Vaccari, A. (1991). *Catal. Today*, 11, 173.
- [8] Chen, X., Fu, C., Wang, Y., Yang, W., & Evans, D. G. (2008). *Biosens. Bioelectron.*, 24, 356.
- [9] Abdolmohammad-Zadeh, H., Rezvani, Z., Sadeghi, G. H., & Zorufi, E. (2011). *Anal. Chim. Acta.*, 685, 212.
- [10] Bocclair, J. W. & Braterman, P. S. (1999). *Chem. Mater.*, 11, 298.
- [11] Li, M., Chen, S., Ni, F., Wang, Y., & Wang, L. (2008). *Electrochim. Acta*, 53, 7255.
- [12] Sels, B. et al. (1999). *Nature*, 400, 855.
- [13] Li, F., Tan, Q., Evans, D., & Duan, X. (2005). *Catal. Lett.*, 99, 151.
- [14] Trifirò, F., & Vaccari, A. (1996). *Comprehensive Supramolecular Chemistry*, Pergamon: Oxford.
- [15] Gardner, C. R. (1985). *Biomaterials*, 6, 153.
- [16] Shichi, T., Takagi, K., & Sawaki, Y. (1996). *Chem. Commun.*, 17, 2027.
- [17] Del Hoyo, C. (2007). *Appl. Clay Sci.*, 36, 103.
- [18] Bish, D. (1980). *Bull. Miner.*, 103, 170.
- [19] Pavan, P. C., Cardoso, L. P., Crepaldi, E. L., & Valim, J. B. (2000). In: *Studies in Surface Science and Catalysis*, Abdelhamid, S., & Mietek, J. (Eds.), Chapter IV Synthesis of other nanoporous and nanostructured materials, Elsevier: The Netherlands, 401.
- [20] Jayashree, R. S., & Vishnu Kamath, P. (2002). *J. Power Sources.*, 107, 120.
- [21] Gérardin, C., Kostadinova, D., Sanson, N., Coq, B., & Tichit, D. (2005). *Chem. Mater.*, 17, 6473.
- [22] Liu, Z. et al. (2006). *J. Am. Chem. Soc.*, 128, 4872.
- [23] Lopez, T. et al. (1996). *Langmuir*, 16, 189.
- [24] Tsai, W. T. et al. (2001). *Chemosphere*, 45, 51.
- [25] Saiah, F. B. D., Su, B. L., & Bettahar, N. (2009). *J. Hazard. Mater.*, 165, 206.
- [26] Kannan, S. (2004). *J. Mater. Sci.*, 39, 6591.
- [27] Oh, J. M., Hwang, S. H., & Choy, J. H. (2002). *Solid State Ion.*, 151, 285.
- [28] Ren, L., Hu, J. S., Wan, L. J., & Bai, C. L. (2007). *Mater. Res. Bull.*, 42, 571.

- [29] Ay, A. N., Zümreoglu-Karan, B., & Temel, A. (2007). *Micropor. Mesopor. Mater.*, 98, 1.
- [30] Bezerra, M. A., Santelli, R. E., Oliveira, E. P., Villar, L. S., & Escaleira, L. A. (2008). *Talanta*, 76, 965.
- [31] Silva, C. G., Bouizi, Y. S., Fornés, V., & Garcí'a, H. (2009). *J. Am. Chem. Soc.*, 131, 13833.
- [32] Nejati, K., & Rezvani, Z. (2012). *J. Exp. Nanosci.*, 7, 412.
- [33] Parida, K., & Mohapatra, L. (2012). *J. Chem. Eng.*, 179, 131.
- [34] Khenifi, A., Derriche, Z., Mousty, C., Prévot, V., & Forano, C. (2010). *Appl. Clay Sci.*, 47, 362.
- [35] Choy, J. H., Park, J. S., Kwak, S. Y., Jeong, Y. J., & Han, Y. S. (2000). *Mol. Cryst. Liq. Cryst.*, 341, 425.
- [36] Seftel, E. M. *et al.* (2008). *Micropor. Mesopor. Mater.*, 113, 296.
- [37] Li, B., He, J., Evans, D. G., & Duan, X. (2006). *J. Phys. Chem. Solids*, 67, 1067.
- [38] Wu, Q. *et al.* (2007). *J. Mater. Chem.*, 17, 965.
- [39] Li, C., Wang, G., Evans, D. G., & Duan, X. (2004). *J. Solid State Chem.*, 177, 4569.
- [40] Klopprogge, J. T., & Frost, R. L. (1999). *J. Solid State Chem.*, 146, 506.
- [41] Tian, Y., Wang, G., Li, F., & Evans, D. G. (2007). *Mater. Lett.*, 61, 1662.